THEORY OF HYPERFINE STRUCTURE OF THE MÖSSBAUER LINE IN PARAMAGNETIC SUBSTANCES

A. M. AFANAS'EV and Yu. KAGAN

Submitted to JETP editor, May 25, 1963

J. Exptl. Theoret. Phys. (U.S.S.R.) 45, 1660-1677 (November, 1963)

The hyperfine structure of a nuclear line in a paramagnetic material in the absence of an external magnetic field is treated. Spin-lattice relaxation of the electronic moment is assumed. A diagram method is developed which gives the explicit form of the appropriate correlation function and hence the absorption spectrum of γ rays in the crystal over a wide temperature range and for an arbitrary ratio of the relaxation frequencies and the characteristic frequencies of the hyperfine interaction. The results are analyzed for limiting cases and for some simple examples, corresponding to an electronic angular momentum $J = {}^3/_2$ and to the case of large electronic angular momentum.

1. INTRODUCTION

THE unique resolution of spectral lines in the Mössbauer effect opened unexpected possibilities for a direct and detailed study of the hyperfine structure of nuclear levels. The structure of the Mössbauer line carries information about the hyperfine interaction in the ground and excited states of the nucleus.

Consider an isolated atom whose electron shell has an uncompensated angular momentum J, and whose nucleus has spin I. The spectrum of such an atom will show a hyperfine structure whose lines are characterized by the value of the conserved total angular momentum.

Suppose that the atoms of this element form an ordered magnetic structure. Then at sufficiently low temperatures the projection of the electronic angular momentum on a particular direction will be an integral of the motion. Once again we get a definite hyperfine structure, whose lines are characterized by the projection of the nuclear spin on the particular direction. The widths of individual Mössbauer lines should be close to the width of the excited nuclear level. This is just the picture which appeared in experiments on the hyperfine structure of the Mössbauer line in ferromagnets and antiferromagnets (cf., for example, [11]).

The situation is drastically changed when an atom with an uncompensated angular momentum of the electron shells is put in a crystal which is not magnetically ordered (either in the form of an impurity or to produce a regular structure). In this case neither the angular momentum of the electron shell nor the total angular momentum of the atom are conserved. As a result of interaction with the external medium, the electronic angular momentum vector suffers random changes with time, and as a result the hyperfine splitting begins to depend on the relaxation properties of the system.

In the limit of long relaxation times the spectrum coincides with the hyperfine structure of the individual atom. In the opposite limit, when the relaxation time is small and the hyperfine interaction is purely magnetic, in the absence of an external magnetic field the hyperfine structure vanishes. Such a picture was observed in the early work of Wertheim,[2] on the Mössbauer effect for Fe^{57} nuclei in paramagnetic stainless steel. The absence of hyperfine structure was also found in the work of Nagle et al,[3] who studied the Mössbauer effect in the paramagnetic alloy PdCo (at very low concentrations of Co).

In the presence of quadrupole interaction (throughout we consider interaction of the nucleus only with its own electron shells), if there is no Stark splitting of the electronic levels in the crystal rapid relaxation results in a similar disappearance of the hyperfine structure. If, however, the interaction of the electron shell with the crystal field leads to a sizable splitting of the Stark levels, the hyperfine structure remains even in the limit of short relaxation time, if the Boltzmann populations of the Stark levels are different. (If the Stark levels are equally populated, i.e., at sufficiently high temperatures, the hyperfine structure disappears in this case also.)

It is obvious that for an arbitrary ratio of the frequencies of relaxation and of the hyperfine

structure we will get a complicated hyperfine splitting which changes rapidly with temperature. This applies to the number of lines as well as to their position and width.

Experimentally the hyperfine structure of Mössbauer lines in paramagnets in the absence of a magnetic field, and its dependence on temperature, was first shown clearly for the oxides of the rare earths.[4-8]

The present paper treats the hyperfine structure of the Mössbauer line in paramagnets with spin-lattice relaxation. A diagram method is developed which gives the absorption spectrum of γ rays in the crystal over a wide temperature range and for an arbitrary ratio of the relaxation frequencies and the characteristic frequencies of the hyperfine interaction.

In addition to a general analysis of the results, we treat various specific cases. We give special attention to situations where it is possible in principle to have a large change in the hyperfine structure without any significant change in the width of the individual lines.

2. DERIVATION OF GENERAL FORMULAS

Suppose that a crystal contains paramagnetic atoms whose nuclei have a low-lying isomeric level E_1. Consider the resonance absorption spectrum of such a system near $\omega_n = E_1 - E_0$, assuming that we have a Mössbauer effect.

We introduce the operator $\hat{d}$, which depends only on the nuclear coordinates and determines the interaction of the γ quanta with the nucleus. Then the absorption spectrum of the system will be determined completely by the real part of the Fourier component of the correlation function:

$$\varphi(t) = \theta(t)\,\mathrm{Sp}\,(\hat{\rho}\hat{d}(t)\hat{d}), \tag{2.1}$$

$$\hat{d}(t) = \exp(i\hat{H}t)\,\hat{d}\exp(-i\hat{H}t), \tag{2.2}$$

where $\hat{\rho}$ is the density matrix and $\hat{H}$ is the total Hamiltonian,

$$\theta(t) = \begin{cases} 1, & t>0 \\ 0, & t<0 \end{cases}$$

(where we set $\hbar = 1$).

We shall assume that the interaction of the nucleus with the surrounding medium, which we denote by H_{hf}, occurs only through its own electronic shells, and has the usual form for the hyperfine interaction for the free ion.

The total Hamiltonian can be written as follows:

$$\hat{H} = \hat{H}_1 + \hat{V} + \hat{H}_0, \qquad \hat{H}_1 = \hat{H}_n + \hat{H}_{hf} + \hat{H}_{cr}. \tag{2.3}$$

Here $\hat{H}_n$ is the Hamiltonian for the nucleus in the absence of hyperfine interaction, $\hat{H}_{cr}$ is the Hamiltonian describing the interaction of the electron shells with the crystal field; $\hat{H}_0$ is the Hamiltonian for the crystal vibrations, and $\hat{V}$ is the spin-lattice interaction which gives rise to the relaxation of the electronic moment.

The expression for $\hat{H}_0$ has the usual form:

$$\hat{H}_0 = \tfrac{1}{2}\sum_\beta \omega_\beta\,(\hat{b}_\beta^+\hat{b}_\beta + \hat{b}_\beta\hat{b}_\beta^+), \tag{2.4}$$

where $\hat{b}_\beta^+$ and $\hat{b}_\beta$ are the operators for creation and annihilation of phonons corresponding to the normal mode β.

Assuming that the spin-lattice relaxation occurs through one-phonon processes, we shall write the expression for $\hat{V}$ in the form

$$\hat{V} = \sum_\beta (\hat{M}_\beta\hat{b}_\beta + \hat{M}_\beta^+\hat{b}_\beta^+), \tag{2.5}$$

where $\hat{M}_\beta$ and $\hat{M}_\beta^+$ are operators acting in the space of eigenfunctions of the operator H_{cr}. (We note that the derivation given below can easily be generalized to the case where multiphonontransitions are important for the relaxation.)

We are interested in the hyperfine structure of the Mössbauer line for an arbitrary ratio of the relaxation time τ_r and the characteristic frequency of the hyperfine interaction ϵ, i.e., for an arbitrary relation between $\hat{V}$ and H_{hf}. On the other hand we shall assume, as usual, that both the conditions

$$\varepsilon \ll \Delta,\ \omega_0,\ T, \tag{2.6}$$

and

$$\Delta\tau_r,\ \omega_0\tau_r,\ T\tau_r \gg 1. \tag{2.7}$$

are satisfied. Here Δ is the characteristic separation of the arbitrarily degenerate levels corresponding to the Hamiltonian $\hat{H}_{cr}$; ω_0 is a characteristic frequency in the phonon spectrum; T is the temperature in energy units.

In accordance with our earlier remarks, in the expression for the density matrix we can drop $\hat{V}$ in the Hamiltonian, so that $\hat{\rho}$ becomes simply the product of two matrices:

$$\hat{\rho} = \hat{\rho}^0\hat{\rho}^1, \qquad \hat{\rho}^{0,1} = \{\mathrm{Sp}\exp(-\hat{H}_{0,1}/T)\}^{-1}\exp(-\hat{H}_{0,1}/T). \tag{2.8}$$

We now proceed to transform (2.1). We use the well known representation of the operator

$$\exp(-i\hat{H}t) = \exp\{-i(\hat{H}_0+\hat{H}_1)t\}\Big\{1 + \sum_{k=1}^{\infty}(-i)^k\int_0^t dt_k\int_0^{t_k} dt_{k-1}\ldots\int_0^{t_2} dt_1\hat{V}(t_k)\hat{V}(t_{k-1})\ldots\hat{V}(t_1)\Big\},$$

$$\hat{V}(t) = \exp\{i(\hat{H}_0+\hat{H}_1)t\}\,\hat{V}\exp\{-i(\hat{H}_0+\hat{H}_1)t\}. \tag{2.9}$$

We introduce the operator

$$\tilde{V}(t) = \exp(i\hat{H}_0 t)\,\hat{V}\exp(-i\hat{H}_0 t). \qquad (2.10)$$

Using the properties of the function $\theta(t)$, it is easy to transform (2.9) to the form

$$\exp(-i\hat{H}t) = \exp(-i\hat{H}_0 t)\{\exp(-i\hat{H}_1 t) + i\sum_{k=1}^{\infty}\int_{-\infty}^{\infty}\ldots\int_{-\infty}^{\infty} dt_k\ldots dt_1\,[-i\theta(t-t_k) \times \exp\{-i\hat{H}_1(t-t_k)\}]\tilde{V}(t_k) \times [-i\theta(t_k - t_{k-1})\exp\{-i\hat{H}_1(t_k - t_{k-1})\}] \times \ldots \tilde{V}(t_1)\,[-i\theta(t_1)\exp(-i\hat{H}_1 t_1)]\}. \qquad (2.11)$$

We can write a completely analogous expansion for $\exp(i\hat{H}t)$.

If we substitute (2.11) in (2.1), the correlation function splits into a sum of terms, each of which can be associated with a simple graph. But the presence of the infinite integration limits allows us to develop directly a diagram technique for the Fourier components of the correlation function, which is very much simpler. It is useful to go to a representation in which $\hat{H}_0$ and $\hat{H}_1$ are diagonal. For the matrix elements of the expressions in the square brackets in (2.11) we can write the following relation:

$$-i\theta(\tau)e^{-iE_j\tau} = \int_{-\infty}^{\infty} G_j(\omega)e^{-i\omega\tau}d\omega, \qquad (2.12)$$

$$G_j(\omega) = \{2\pi(\omega - E_j + i\delta)\}^{-1}. \qquad (2.13)$$

The expansion of $\exp(i\hat{H}t)$ contains factors of the form $i\theta(\tau)\exp(iE_j\tau)$, for which we have in place of (2.12)

$$i\theta(\tau)e^{iE_j\tau} = \int_{-\infty}^{\infty} G_j^*(\omega)e^{i\omega\tau}d\omega, \qquad (2.14)$$

where $G_j^*(\omega)$ is the complex conjugate of (2.13).

The Fourier component $\varphi(\omega)$ of the correlation function (2.1) splits into a sum of terms, to each of which we can associate a graph of the type shown in Fig. 1. Since the transition to the Fourier representation is straightforward, we shall limit ourselves to simply formulating the rules for drawing individual graphs.

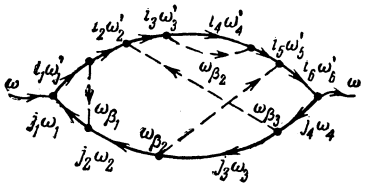

FIG. 1

1. The number of points on a solid line going from left to right corresponds to the number of operators $\hat{V}$ in the expansion (2.11), and the number of points on a solid line going from right to left is determined by the number of operators $\hat{V}$ in the corresponding expansion of $\exp(i\hat{H}t)$.

2. To each line segment between two points, going left to right, there corresponds a factor $G_j(\omega)$ (2.13), and to one going from right to left, a factor $G_j^*(\omega)$.

3. In summing over the phonon variables in the expression for the correlation function, taking account of the expression for the density matrix (2.8), the only nonzero contributions are from those terms in which the phonon creation and annihilation operators appearing in each factor $\hat{V}$ [cf. (2.5)] are paired.

Accordingly, all the points on the solid lines should be joined in pairs in all possible ways by the dashed phonon lines. To each dashed line there corresponds a factor n_{β_k}, if the phonon line emerges from a point on the lower curve and ends either on the upper curve or on a point of the lower curve lying to the right, or if the dashed line emerges from a point of the upper curve and ends in a point of the upper curve lying to the left. In all other cases the factor corresponding to a dashed line is of the form $n_{\beta_k} + 1$.

In each term $\varphi(\omega)$ corresponding to a specific graph, there is an explicit averaging over the equilibrium phonon distribution. Because of the quasi-continuous nature of the phonon spectrum, s such an averaging is given to macroscopic accuracy by replacing n_{β_k} by $\bar{n}_{\beta_k}$.

4. To each point on the lower curve at the junction of lines with indices j_k and j_{k+1}, there corresponds the factor

$$(M_{\beta_k}^{+})_{j_{k+1}}^{j_k}\cdot 2\pi\delta(\omega_{k+1} - \omega_k - \omega_{\beta_k}),$$

if the phonon line emerges from the point, and the factor

$$(M_{\beta})_{j_{k+1}}^{j_k}\cdot 2\pi\delta(\omega_{k+1} - \omega_k + \omega_{\beta_k}),$$

if the phonon line ends at the point. Similarly, for a point on the upper curve at the junction of lines with indices i_k and i_{k+1} we have, respectively,

$$(M_{\beta_k}^{+})_{i_k}^{i_{k+1}}\cdot 2\pi\delta(\omega_k' - \omega_{k+1}' - \omega_{\beta_k}),$$

$$(M_{\beta_k})_{i_k}^{i_{k+1}}\cdot 2\pi\delta(\omega_k' - \omega_{k+1}' + \omega_{\beta_k}).$$

5. To the left vertex there corresponds the factor $d_{j_1}^{i_1}(\hat{\rho}^1)_{j_1}^{j_1}$, to the right vertex, $d_{i_m}^{j_n}\cdot 2\pi\times\delta(\omega_{j_n} - \omega_{i_m}' + \omega)$.

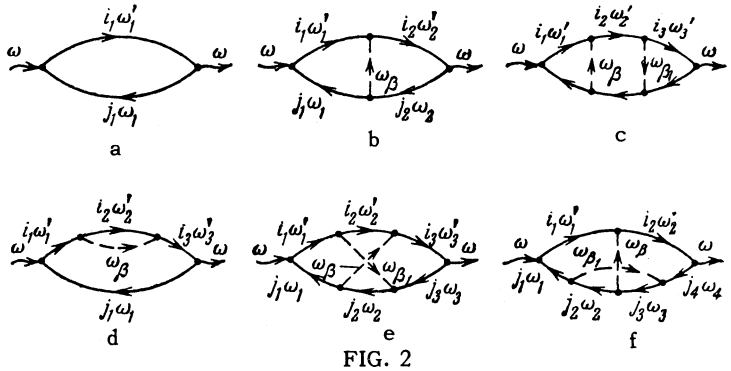

FIG. 2

6. For all frequencies ω_k and ω'_k there is an integration between the limits $-\infty$ and $+\infty$, and for all subscripts β_k there is a summation over the quasicontinuous phonon spectrum. In addition there is a summation over the indices i_k, j_k, running through the finite number of values corresponding to the levels of the Hamiltonian $\hat{H}_1$.

If we fix the frequencies of the phonon lines, $\omega_{\beta k}$, then we can integrate explicitly over all the frequencies ω_k, ω'_k, except one. This integration removes all the δ functions.

Now let us consider the graphs shown in Fig. 2. To graph a there corresponds the expression

$$\sum_{i_1, j_1} \hat{d}^{j_1}_{i_1}\hat{d}^{i_1}_{j_1}(\hat{\rho}^1)^{j_1}_{j_1}\frac{1}{2\pi}\int\!\!\int_{-\infty}^{\infty}\frac{1}{\omega'_1 - E_{i_1}+i\delta}\,\frac{1}{\omega_1 - E_{j_1}-i\delta}$$

$$\times\,\delta(\omega'_1-\omega_1-\omega)\,d\omega_1 d\omega'_1$$

$$=\sum_{i_1, j_1}\hat{d}^{j_1}_{i_1}\hat{d}^{i_1}_{j_1}(\hat{\rho}^1)^{j_1}_{j_1}\frac{i}{\omega - E_{i_1}+E_{j_1}+i\delta}. \qquad (2.15)$$

We shall be interested in the shape of the spectral line in the vicinity of the nuclear transition, at distances of the order of the hyperfine interaction ϵ, i.e.,

$$|\omega-\omega_n|\sim\varepsilon. \qquad (2.16)$$

But before proceeding with the analysis, let us look at the structure of the levels E_j and E_i corresponding to the Hamiltonian H_1 (E_j describes the set of levels corresponding to the nuclear ground state, and E_i those for the excited state).

The ground state levels will be characterized by two indices m,f, where m characterizes the arbitrarily degenerate Stark level E_m, while the set of quantum numbers f is determined by the Hamiltonian for the hyperfine interaction. Similarly the levels for the excited state will be characterized by indices m and g (Obviously the hyperfine structure depends essentially on the state of the nucleus, so that the sets of quantum numbers f and g are different.)

Thus the expressions for E_i and E_j can be written as follows:

$$E_j\equiv E_{nf}=E_n+\varepsilon_{nf},\qquad E_i\equiv\omega_n+E_{mg}=\omega_n+E_m+\varepsilon_{mg}. \qquad (2.17)$$

Since the separation of Stark levels is large compared to the hyperfine splitting (cf. (2.6)), taking account of (2.16) and (2.17) we have

$$[\omega-E_i+E_j+i\delta]^{-1}=\delta_{nm}\,[(\omega-\omega_n)-\varepsilon_{mg}+\varepsilon_{mf}+i\delta]^{-1} \qquad (2.18)$$

For graph b, if we first perform the trivial integration over ω'_1 and ω'_2, we have

$$\sum_{i_1 j_1 i_2 j_2}\hat{d}^{j_1}_{i_2}\hat{d}^{i_1}_{j_1}(\hat{\rho}^1)^{j_1}_{j_1}\frac{1}{(2\pi)^2}\int\!\!\int_{-\infty}^{\infty}d\omega_1 d\omega_2\,\frac{1}{\omega_1+\omega-E_{i_1}+i\delta}\,\frac{1}{\omega_1-E_{j_1}-i\delta}$$
$$\times\,\frac{1}{\omega_2+\omega-E_{i_2}+i\delta}\,\frac{1}{\omega_2-E_{j_2}-i\delta}$$
$$\times\sum_{\beta}2\pi\,(\hat{M}^+_\beta)^{j_1}_{j_2}(\hat{M}_\beta)^{i_2}_{i_1}\bar{n}_\beta\delta\,(\omega_\beta-\omega_2+\omega_1). \qquad (2.19)$$

The expression $[\omega_k+\omega-E_{i_k}+i\delta]^{-1}\times[\omega_k-E_{j_k}-i\delta]^{-1}$ as a function of ω_k for $n_k=m_k$, has a sharp maximum in the neighborhood of $\omega_k=E_{j_k}$ with a width of order ϵ. If we use (2.6), it is natural to assume that all quantities depending on the phonon spectrum hardly change over an energy interval of order ϵ. Then we can replace ω_1 by E_n and ω_2 by E_{n_2} in the δ function under the summation sign in (2.19), after which the integration over ω_1 and ω_2 is elementary.

If however $n_k\neq m_k$, one can easily verify that for each frequency the integration gives a small factor $\sim\epsilon/\Delta$ compared to the case where $n_k=m_k$, so we can neglect the corresponding terms in the sum (2.19).

As a result the final expression for graph b can be written in the form

$$\sum_{i'_1 j_1 i_2 j_2}d^{j_2}_{i_2}d^{i_1}_{j_1}(\hat{\rho}^1)^{j_1}_{j_1}\frac{i\delta_{n_1 m_1}}{\omega-E_{i_1}+E_{j_1}+i\delta}$$
$$\times\left(\sum_\beta 2\pi\,(M^+_\beta)^{j_1}_{j_2}(M_\beta)^{i_2}_{i_1}\bar{n}_\beta\delta\,(\omega_\beta-E_{n_2}+E_{n_1})\right)$$
$$\times\,\frac{i\delta_{n_2 m_2}}{\omega-E_{i_2}+E_{j_2}+i\delta}. \qquad (2.20)$$

Proceeding in exactly similar fashion, one can easily find the expression corresponding to graph c:

$$\sum_{i_1 j_1 i_2 j_2 i_3 j_3} d^{j_3}_{i_3} d^{i_1}_{j_1} (\hat{\rho}^1)^{j_1}_{i_1} \frac{i\delta_{n_1 m_1}}{\omega - E_{i_1} + E_{j_1} + i\delta} \times \left(\sum_{\beta} 2\pi \, (M^+_\beta)^{j_1}_{j_2} (M_\beta)^{i_2}_{i_1} \bar{n}_\beta \delta \, (\omega_\beta - E_{n_2} + E_{n_1}) \right) \times \frac{i\delta_{n_2 m_2}}{\omega - E_{i_2} + E_{j_2} + i\delta} \times \left(\sum_{\beta_1} 2\pi \, (M_{\beta_1})^{j_2}_{j_3} (M^+_{\beta_1})^{i_3}_{i_2} (\bar{n}_{\beta_1} + 1) \, \delta \, (\omega_{\beta_1} + E_{n_3} - E_{n_2}) \right) \times \frac{i\delta_{n_3 m_3}}{\omega - E_{i_3} + E_{j_3} + i\delta} \cdot \tag{2.21}$$

For diagram d, dropping the integrals over ω'_1, ω'_2, ω'_3, by using the corresponding δ functions, we have

$$\sum_{i_1 i_2 i_3 j_1} d^{j_1}_{i_3} d^{i_1}_{j_1} (\hat{\rho})^{j_1}_{j_1} \frac{1}{2\pi} \times \int \frac{1}{\omega_1 + \omega - E_{i_1} + i\delta} \frac{1}{\omega_1 + \omega - E_{i_3} + i\delta} \frac{1}{\omega_1 - E_{j_1} - i\delta} \times \sum_{\beta} (M_\beta)^{i_3}_{i_2} (M^+_\beta)^{i_2}_{i_1} (\bar{n}_\beta + 1) \frac{d\omega_1}{\omega_1 + \omega - \omega_\beta - E_{i_2} + i\delta} \cdot$$

The resulting integral is computed by elementary methods using residues. The final result is conveniently written as

$$\sum_{i_1 j_1 i_2 j_2} d^{j_2}_{i_2} d^{i_1}_{j_1} (\hat{\rho}^1)^{j_1}_{i_1} \frac{i}{\omega - E_{i_1} + E_{j_1} + i\delta} \times \left[-i \sum_{\beta, \, i_3} \delta^{j_1}_{j_2} \frac{(M_\beta)^{i_2}_{i_3} (M^+_\beta)^{i_3}_{i_1} (\bar{n}_\beta + 1)}{\omega - E_{i_3} + E_{j_1} - \omega_\beta + i\delta} \right] \times \frac{i}{\omega - E_{i_2} + E_{j_2} + i\delta} \cdot \tag{2.22}$$

Diagram e corresponds to the expression

$$(2\pi)^3 \sum_{i_1 j_1 i_2 j_2 i_3 j_3} d^{j_3}_{i_3} d^{i_1}_{j_1} (\hat{\rho}^1)^{j_1}_{j_1} \times \int_{-\infty}^{\infty} d\omega_1 d\omega_2 d\omega_3 G_{i_1}(\omega_1 + \omega) \, G^*_{j_1}(\omega_1) \, G_{i_3}(\omega_3 + \omega) \, G^*_{j_3}(\omega_3) \times G_{i_2}(\omega_1 + \omega_3 + \omega - \omega_2) \, G^*_{j_2}(\omega_2) \sum_{\beta\beta_1} (2\pi)^2 \delta(\omega_1 + \omega_\beta - \omega_2) \times \delta(\omega_3 - \omega_2 + \omega_{\beta_1}) \times (M^+_\beta)^{j_1}_{j_2} (M_\beta)^{j_2}_{j_3} (M_\beta)^{i_3}_{i_2} (M^+_{\beta_1})^{i_2}_{i_1} \bar{n}_\beta (\bar{n}_{\beta_1} + 1).$$

The same arguments as in the derivation of (2.20) from (2.19) allow us to do the integration over ω_1, ω_3:

$$2\pi \sum_{i_1 j_1 i_2 j_2 i_3 j_3} d^{j_3}_{i_3} d^{i_1}_{j_1} (\hat{\rho}^1)^{j_1}_{j_1} \frac{i\delta_{n_1 m_1}}{\omega - E_{i_1} + E_{j_1} + i\delta} \frac{i\delta_{n_3 m_3}}{\omega - E_{i_3} + E_{j_3} + i\delta} \times \int_{-\infty}^{\infty} d\omega_2 G_{i_2}(E_{j_1} + E_{j_3} + \omega - \omega_2) \, G^*_{j_2}(\omega_2) \times \left[\sum_{\beta\beta_1} (2\pi)^2 \delta(E_{j_1} + \omega_\beta - \omega_2) \, \delta(E_{j_3} - \omega_2 + \omega_{\beta_1}) (M^+_\beta)^{j_1}_{j_2} \times (M_{\beta_1})^{j_2}_{j_3} (M_\beta)^{i_3}_{i_2} (M^+_{\beta_1})^{i_2}_{i_1} \bar{n}_\beta (\bar{n}_{\beta_1} + 1) \right]. \tag{2.23}$$

Now let us analyze the remaining integral. It is easy to see that

$$\int_{-\infty}^{\infty} d\omega_2 G_{i_2}(E_{j_1} + E_{j_3} + \omega - \omega_2) \, G^*_{j_2}(\omega_2) \equiv 0 \tag{2.24}$$

because the poles of both functions lie in the upper halfplane. The expression in square brackets in (2.23), as a function of ω_2, is different from zero over an interval of order ω_0, Δ, and at low temperatures over an interval of order T, and varies smoothly over this interval. Taking this into account as well as (2.24) and the fact that the expression in square brackets in (2.23) is of order τ_r^{-2}, it is easy to show that the integral in (2.23) is of order

$$\tau_r^{-1} \{1/\tau_r\omega_0, \; 1/\tau_r\Delta, \; 1/\tau_r T\}. \tag{2.25}$$

Comparing (2.23) with (2.20), using (2.25) and the initial conditions (2.7), we verify that the contribution of graph e can be neglected. A similar situation occurs whenever intersecting dashed lines occur in a graph (in particular in graphs of the type of f). Thus, in summing over all graphs we shall take only those to which there correspond nonintersecting phonon lines. It turns out that the diagrams of this type can be summed exactly.[1)]

From the form of (2.15), (2.18), (2.20), and (2.21) it follows immediately that the set of all graphs with vertical phonon lines sums to the following expression:

$$\sum_{mfgm_1f_1g_1} \hat{d}^{f_1}_{g_1} \hat{d}^{g}_{f} (\hat{\rho}^1)^{m}_{m} \hat{\Gamma}^{mfg}_{m_1 f_1 g_1}, \tag{2.26}$$

$$\hat{\Gamma} = [-i(\omega - \omega_n)\hat{E} + i\hat{\Omega} - \hat{P}_0]^{-1}, \tag{2.27}$$

where $\hat{E}$ is the unit matrix;

$$\hat{\Omega}^{mfg}_{m_1 f_1 g_1} = -(\varepsilon_{mf} - \varepsilon_{mg}) \delta^{mfg}_{m_1 f_1 g_1}, \tag{2.28}$$

$$\hat{P}_0{}^{mfg}_{m_1 f_1 g_1} = 2\pi \sum [(\hat{M}^+_\beta)^{mf}_{m_1 f_1} (\hat{M}_\beta)^{m_1 g_1}_{mg} \bar{n}_\beta \delta(E_m - E_{m_1} + \omega_\beta) + (\hat{M}_\beta)^{mf}_{m_1 f_1} (\hat{M}^+_\beta)^{m_1 g_1}_{mg} (\bar{n}_\beta + 1) \, \delta(E_m - E_{m_1} - \omega_\beta)]. \tag{2.29}$$

In writing (2.26) we have neglected the hyperfine interaction energy compared to T, so that

[1)] In the summation we also drop diagrams which have dashed lines joining two points on the same solid line which have other points lying between them. These diagrams are of the same order as diagrams e and f.

the density matrix $\hat{\rho}^1$ depends only on the index m characterizing the electronic levels.

If we consider the set of graphs containing only horizontal phonon lines on either the upper or the lower solid line, the sum is given similarly to (2.26) and (2.27), with $\hat{P}_0$ replaced by $\hat{P}_1$ or $\hat{P}_2$, where the matrix elements of $\hat{P}_1$, in accordance with (2.22), are given by

$$\hat{P}_{1m_1f_1g_1}^{mfg} = -i\sum_{m_2g_2\beta}\delta_{m_1f_1}^{mf}((\hat{M}_\beta)_{m_2g_2}^{m_1g_1}(\hat{M}_\beta^+)_{mg}^{m_2g_2}(\bar{n}_\beta+1)\times[E_m-E_{m_2}-\omega_\beta+i\delta]^{-1}+(\hat{M}_\beta^+)_{m_2g_2}^{m_1g_1}(\hat{M}_\beta)_{mg}^{m_2g_2}\bar{n}_\beta[E_m-E_{m_2}+\omega_\beta+i\delta]^{-1}). \quad (2.30)$$

For $\hat{P}_2$ we have the analogous expressions:

$$\hat{P}_{2m_1f_1g_1}^{mfg} = i\sum_{m_2f_2\beta}\delta_{m_1g_1}^{mg}((\hat{M}_\beta)_{m_2f_2}^{mf}(\hat{M}_\beta^+)_{m_1f_1}^{m_2f_2}(\bar{n}_\beta+1)\times[E_m-E_{m_2}-\omega_\beta-i\delta]^{-1}+(\hat{M}_\beta^+)_{m_2f_2}^{mf}(\hat{M}_\beta)_{m_1f_1}^{m_2f_2}\bar{n}_\beta[E_m-E_{m_2}+\omega_\beta-i\delta]^{-1}). \quad (2.31)$$

It is easy to verify directly that the set of graphs with nonintersecting phonon lines, which determines $\varphi(\omega)$ in this approximation, will be described by the expression

$$\varphi(\omega) = \sum_{mfgm_1f_1g_1}\hat{d}_{g_1}^{f_1}\hat{d}_f^g(\hat{\rho}^1)_m^m\hat{\Gamma}_{m_1f_1g_1}^{mfg}, \quad (2.32)$$

$$\hat{\Gamma} = [-i(\omega-\omega_n)\hat{E}+i\hat{\Omega}-\hat{P}]^{-1}, \quad (2.33)$$

$$\hat{P} = \hat{P}_0+\hat{P}_1+\hat{P}_2. \quad (2.34)$$

The expressions (2.32), (2.33), and (2.28-2.31) completely solve the problem. The spectrum for recoilless emission (absorption) of γ quanta in a paramagnet will be given in the general case by the real part of (2.32).

3. ANALYSIS OF RESULTS

In many cases a direct analysis of the results is conveniently done by going over from the Fourier components of the correlation function to the correlation function $\varphi(t)$ itself. For the latter, using (2.32), we find

$$\varphi(t) = \theta(t)e^{-i\omega_n t}\sum_{mfgm_1f_1g_1}\hat{d}_{g_1}^{f_1}\hat{d}_f^g(\hat{\rho}^1)_m^m\{\exp[(-i\hat{\Omega}+\hat{P})t]\}_{m_1f_1g_1}^{mfg}. \quad (3.1)$$

The expression (3.1) can easily be written as the trace of a product of operators defined in the space

$$L = \sum_m L_m^0\times L_m^1, \quad (3.2)$$

where L_m^0 and L_m^1 are the spaces formed respectively by the functions $|mf\rangle$ and $|mg\rangle$ (with m fixed). This allows us, in calculating the correlation function, to use a different representation, N, which is related to (3.2) by a unitary transformation. Let us use m, p for the set of quantum numbers characterizing H_{cr} and belonging to the degenerate level m, and the indices M, I for the projections of the nuclear angular momentum on some selected direction in the ground and excited states, respectively.

Let N_m^0 and N_m^1 be the spaces formed by the states

$$|mpM\rangle = |mp\rangle|M\rangle, \qquad |mpI\rangle = |mp\rangle|I\rangle.$$

Then

$$N = \sum_m N_m^0\times N_m^1. \quad (3.2')$$

In this representation

$$\varphi(t) = \theta(t)e^{-i\omega_n t}\sum_{mm_1pp_1\sigma\sigma_1}\hat{D}_\sigma^{\sigma_1}(\hat{\rho}^1)_m^m\{\exp[(-i\hat{\Omega}+\hat{P})t]\}_{m_1p_1p_1\sigma_1}^{mpp\sigma}. \quad (3.3)$$

Here σ is the set of quantum numbers $\{M, I\}$:

$$\hat{D}_\sigma^{\sigma_1} \equiv \hat{D}_{MI}^{M_1I_1} = \hat{d}_{I_1}^{M_1}\hat{d}_M^I. \quad (3.3')$$

In this representation the operator $\hat{P}$ has a very simple form—it is diagonal in the quantum numbers σ (if, as is natural, we neglect the effect of the hyperfine interaction on the relaxation of the electron spin):

$$\hat{P}_{m_1p_1q_1\sigma_1}^{mpq\sigma} = \hat{\tilde{P}}_{m_1p_1q_1}^{mpq}\delta_{\sigma_1}^{\sigma}. \quad (3.4)$$

The formulas giving the matrix elements $\hat{\tilde{P}}_{m_1p_1q_1}^{mpq}$ are exactly analogous to formulas (2.34), (2.29)—(2.31), and are obtained from them by replacing the indices m_if_i and m_ig_i by m_ip_i and m_iq_i. If in the expressions

$$\frac{1}{E_m-E_{m_2}\pm\omega_\beta\pm i\delta} = P\frac{1}{E_m-E_{m_2}\pm\omega_\beta}\mp i\pi\delta(E_m-E_{m_2}\pm\omega_\beta),$$

which appear in formulas (2.20) and (2.31) we neglect the principal part (or assign the expressions given by the principal part to the operator $\hat{\Omega}$), $\hat{\tilde{P}}$ can easily be shown to have the following properties:

$$\sum_{np_1}\hat{\tilde{P}}_{np_1p_1}^{mpq} = 0, \quad (3.5)$$

$$\hat{\tilde{P}}_{np_1q_1}^{mpq} = \exp[(E_m-E_n)/T]\hat{\tilde{P}}_{mpq}^{np_1q_1}, \quad (3.6)$$

$$\sum_{mp}(\hat{\rho}^1)_m^m\hat{\tilde{P}}_{np_1q_1}^{mpp} = 0. \quad (3.7)$$

The matrix elements of the operator $\hat{\Omega}$ are given by the formulas

$$\hat{\Omega}^{mpq\sigma}_{m_1p_1q_1\sigma_1} = -[(H^0_{\rm hf})^{mpM}_{m_1p_1M_1}\delta^{mqI}_{m_1q_1I_1} - (H^1_{\rm hf})^{m_1q_1I_1}_{mqI}\delta^{mpM}_{m_1p_1M_1}]. \quad (3.8)$$

We recall that H^0_{hf} and H^1_{hf} are the operators for the hyperfine interaction in the ground and excited states of the nucleus.

Now let us analyze the expressions (3.1) and (3.2) for the correlation function. This analysis can be carried out most simply in general form for two limiting cases: 1) when all the relaxation frequencies are small compared to the frequencies in the hyperfine structure ($\tau_r\epsilon \gg 1$); 2) when the relaxation frequencies are large compared to the frequencies of the hyperfine structure ($\tau_r\epsilon \ll 1$).

In the first case we use (3.1) in which we neglect $\hat{P}$ compared to $\hat{\Omega}$. Then, using (2.28), we find

$$\varphi(t) = \theta(t)\, e^{-i\omega_n t}\sum_{mfg}|\hat{d}^{mf}_{mg}|^2\frac{\exp(-E_m/T)}{\sum_{mf}\exp(-E_m/T)}e^{-i\omega_{mfg}t},$$
$$\omega_{mfg} = \varepsilon_{mf} - \varepsilon_{mg}. \quad (3.9)$$

For $t > 0$ the expression (3.9) is just a sum of exponentials. Thus the absorption (emission) spectrum will consist of a set of very narrow lines with frequencies $\omega_n \sim \epsilon_{mf} + \epsilon_{mg}$ (the widths of the individual lines will be the natural width of the first excited state of the nucleus).

Suppose that $T \ll \Delta$ and consequently only the first electronic level is excited. Then the hyperfine structure consists of a single "flag" with a number of lines equal to the number of allowed transitions. As the temperature increases, a second flag begins to develop, corresponding to the next electronic level, and so with increasing temperature we get successively the flag patterns for all the hyperfine lines corresponding to different m. Thus in this case so long as the condition $\hat{P} \ll \hat{\Omega}$ is satisfied, the absorption spectrum of the γ quanta will be a superposition of flag patterns of hyperfine lines, and the spectrum will change rapidly with temperature until we reach $T \sim Em_{max}$.

If we cannot drop $\hat{P}$ compared to $\hat{\Omega}$ in (3.1), then to find the spectral density of absorption of γ quanta it is useful first to transform the matrix $-i\hat{\Omega} + \hat{P}$ to diagonal form. Then (3.1) splits into a sum of exponentials:

$$\varphi(t) = \theta(t)\, e^{-i\omega_n t}\sum_k A_k e^{\lambda_k t}, \quad (3.10)$$

where λ_k is a root of the equation

$$|-i\hat{\Omega} + \hat{P} - \lambda\hat{E}| = 0; \quad (3.11)$$

A_k depends on the components of the matrix which accomplishes the transition to the diagonal form.

When the relaxation frequencies are finite but still small compared to the frequencies of the hyperfine structure, the eigenvalues of (3.11) can be found using standard perturbation theory:

$$\lambda_k = -i\omega_k + \hat{P}^k_k + i\sum_{k_1}{}' \frac{\hat{P}^k_{k_1}\hat{P}^{k_1}_k}{\omega_k - \omega_{k_1}}, \quad (3.12)$$

where $k = \{mfg\}$. From (3.12) it follows that the renormalization of the frequency is a quantity of second order in the elements of the matrix $\hat{P}$, if, as is usually the case, $\mathrm{Im}\,\hat{P} \ll \hat{P}$, whereas the smearing out of the line, which is determined by $\mathrm{Re}\,\lambda_k$, is a quantity of first order.

If we make the natural assumption that the relaxation times drop with increasing temperature, then we can conclude that with increasing T the widths of the individual lines increase much more rapidly than the shift.

In the opposite limiting case when $\hat{P} \gg \hat{\Omega}$, it is convenient to use the expression for $\varphi(t)$ in the form (3.3). Now we must use perturbation theory for $\hat{\Omega}$. From (3.4) it follows that the eigenvalues of the operator $-i\hat{\Omega} + \hat{P}$ can be written in the form

$$\lambda_{k\alpha} = \lambda^0_k + i\lambda^1_{k\alpha}, \quad (3.13)$$

where λ^0_k are the eigenvalues of the operator $\hat{P}$, and $\lambda^1_{k\alpha}$ are corrections to λ^0_k due to the operator $\hat{\Omega}$, which tend to zero if $\hat{\Omega}$ goes to zero.

Let us set $\hat{\Omega} \equiv 0$. Then we easily find from (3.5) or (3.7) that

$$\sum_{mpnp_1}(\hat{\rho}^1)^m_m[\exp(\hat{P}t)]^{mpp\sigma}_{np_1p_1\sigma} = 1. \quad (3.14)$$

This means that only one root of (3.11) appears in $\varphi(t)$, namely $\lambda_0 = 0$, and all the coefficients with $k \neq 0$ in (3.10) are zero. For finite $\hat{\Omega}$, under the condition $\hat{\Omega} \ll P$, the expression for $\varphi(t)$ obviously can be written as follows:

$$\varphi(t) = \theta(t)\, e^{-i\omega_n t}\sum_\alpha A_{0\alpha}\exp(i\lambda^1_{0\alpha}t). \quad (3.15)$$

It is easily verified by solving the corresponding secular equation that the quantities $\lambda^1_{0\alpha}$ are the eigenvalues of the matrix

$$\overline{\Omega}^\sigma_{\sigma_1} = -\sum_{mpp_1}(\hat{\rho}^1)^m_m\,\Omega^{mpp\sigma}_{mp_1p_1\sigma_1}. \quad (3.16)$$

Using formula (3.8) we can transform this expression to

$$\overline{\Omega}^{MI}_{M_1I_1} = \sum_{mp}(\hat{\rho}^1)^m_m[(H^0_{\rm hf})^{mpM}_{mpM_1}\delta^I_{I_1} - (H^1_{\rm hf})^{mpI_1}_{mpI}\delta^M_{M_1}]. \quad (3.17)$$

One can verify directly that in this case

$$\varphi(t) = \theta(t)\, e^{-i\omega_n t}\sum_{\sigma_1\sigma}\hat{D}^{\sigma_1}_\sigma[\exp(i\overline{\Omega}t)]^\sigma_{\sigma_1}, \quad (3.18)$$

where the operator $\hat{D}$ is defined by formula (3.3′).

It follows from (3.16)—(3.18) that in the case of very fast relaxation the hyperfine structure of the line appears as a single flag pattern, corresponding to the average of the nuclear interaction with the electron shell of the atom over the Stark levels weighted with the Boltzmann factor. The magnetic part of the interaction averages out completely and only the averaged quadrupole interaction remains. The latter is in general different from zero, but goes to zero as one approaches equal population of the Stark levels (cf. the corresponding discussion in [9]). (This statement is valid if the electric field gradient at the nucleus is due to the electrons in the same atom only. In general at high temperatures there remains the part of the quadrupole interaction caused by the external surroundings.)

The limiting cases considered could be analyzed easily without knowing the specific form of $H_1 = H_{cr} + H_{hf}$. If, however, we want to see the effects of temperature dependence of the hyperfine structure, the most interesting case is the intermediate one, which covers a wide temperature range. The general analysis simplifies considerably if we make simplifying assumptions about the form of H_1. We shall show this for the case considered below.

First we shall assume that the operator $\hat{\Omega}$ is diagonal in the representation (3.28). This situation may be realized in specific cases if, for example, the interaction of the electron shells with the crystal field has the form

$$H_{cr} = F(\hat{J}_z^2), \tag{3.19}$$

and the hyperfine interaction is

$$H_{hf}^i = A^i \hat{J}_z \hat{I}_z. \tag{3.20}$$

Here $\hat{J}_Z$ and $\hat{I}_Z$ are the operators for the projections of the total angular momentum of the electron shell and the nucleus.

The matrix elements $\hat{\tilde{P}}^{mpq}_{np_1q_1}$ with $p \neq q$ or $p_1 \neq q_1$ are a product of matrix elements corresponding to transitions with different multiplicities, averaged over all possible directions of the wave vector and the polarization vectors of the phonons of a given energy. In particular problems these matrix elements may turn out to be small. In this case we may set these matrix elements equal to zero and consider only the matrix elements

$$\hat{\tilde{P}}^{mpp}_{np_1p_1} \equiv \hat{P}^{mp}_{np_1}. \tag{3.21}$$

In accordance with (3.5)—(3.7),

$$\sum_{np_1} \hat{P}^{mp}_{np_1} = 0, \qquad \sum_{mp} (\hat{\rho}^1)^m_m \hat{P}^{mp}_{np_1} = 0, \tag{3.22}$$
$$\hat{P}^{np_1}_{mp} = \exp((E_n - E_m)/T)\, \hat{P}^{mp}_{np_1}.$$

Because of (3.21) and (3.22), the expression for $\varphi(t)$ reduces to

$$\varphi(t) = \theta(t)\, e^{-i\omega_n t} \sum_{mpnp_1MI} |d_I^M|^2 (\hat{\rho}^1)^m_m \times \{\exp[(-i\hat{\Omega}(M, I) + \hat{P})t]\}^{mp}_{np_1}, \tag{3.23}$$

$$\hat{\Omega}(MI) = -(A^0 M - A^1 I)\hat{J}_z. \tag{3.24}$$

The expression (3.23) can be obtained independently by a method similar to the random phase method developed by Anderson.[10] The treatment of the present paper thus enables us to establish the assumptions whose validity is required for the semiclassical random phase method. In the present case the use of (3.23) requires the validity of the initial conditions (2.6) and (2.7), which is essentially the assumption that only the elements (3.21) of the operator $\hat{\tilde{P}}$ are different from zero, and the choice of Hamiltonians H_{cr} and H_{hf} of the type of (3.19) and (3.20).

4. HYPERFINE STRUCTURE OF A NUCLEAR LINE IN A PARAMAGNET. THE CASE OF ELECTRONIC ANGULAR MOMENTUM J = 3/2.

In this section we shall study the character of the hyperfine structure of a nuclear line in a paramagnet for the example of an atom with angular momentum J = 3/2 for its electronic shell. As will be seen from the presentation, the analysis of this case makes it possible to get a complete qualitative picture. For simplicity we shall make the same assumptions as in arriving at (3.23). The system of levels in the crystal field is that shown in Fig. 3.

We introduce the nondegenerate linear operator $\hat{U}$, which brings the matrix $-\hat{\Omega} + \hat{P}$ to diagonal form. Then (3.23) is easily transformed to the following form:

$$\varphi(t) = \theta(t)\, e^{-i\omega_n t} \sum_{MI} |d_I^M|^2 \times \left\{\sum_{ij} (\hat{\rho}^1)^i_i [\hat{U}^{-1} \exp[\hat{U}(-i\hat{\Omega}(MI) + \hat{P})t\hat{U}^{-1}]\hat{U}]^i_j\right\}$$
$$= \theta(t)\, e^{-i\omega_n t} \sum_{MI} \left| d_I^M \right|^2 \left\{\sum_k A_k e^{\lambda_n t}\right\}, \tag{4.1}$$

where the λ_k are the roots of the characteristic determinant (3.11),

$$A_k = \sum_{ij} (\hat{\rho}^1)^i_i (\hat{U}^{-1})^i_k \hat{U}^k_j \tag{4.2}$$

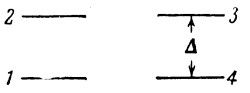

FIG. 3

(i and j label all the states of the electron spin in the notation of Fig. 3.

We write the determinant (3.11) in explicit form:

$$\begin{vmatrix} -i\omega_1 + P_{11} - \lambda & P_{12} & P_{13} & P_{14} \\ P_{21} & -i\omega_2 + P_{22} - \lambda & P_{23} & P_{31} \\ P_{31} & P_{23} & i\omega_2 + P_{33} - \lambda & P_{21} \\ P_{14} & P_{13} & P_{12} & i\omega_1 + P_{44} - \lambda \end{vmatrix} = 0. \tag{4.3}$$

Here we have made use of the obvious equalities for the matrix elements of $\hat{P}$ for the level scheme of Fig. 3:

$$P_{14} = P_{41}, \quad P_{24} = P_{31},$$
$$P_{32} = P_{23}, \quad P_{34} = P_{21}, \quad P_{42} = P_{13}, \tag{4.4}$$

and also, because of (3.24), set

$$\omega_1 \equiv [\hat{\Omega}(MI)]_1^1 = -[\hat{\Omega}(MI)]_4^4,$$
$$\omega_2 \equiv [\hat{\Omega}(MI)]_2^2 = -[\hat{\Omega}(MI)]_3^3.$$

In addition the conditions (3.22) are imposed on the elements P_{ij}, which together with (4.4) give

$$P_{11} = P_{44}, \quad P_{22} = P_{33}. \tag{4.5}$$

A. To begin with, let us consider the picture when the levels are inverted, i.e., when the lower states correspond to $J_Z = \pm 3/2$. Suppose that over a certain temperature range $P_{23} \gg \omega_1, \omega_2$, while all other nondiagonal matrix elements of $\hat{P}$ are small compared to ω_1, ω_2 (only when the population is inverted is it reasonable to assume that $P_{23} \gg P_{14}$). Then we find approximately for the roots of (4.3)

$$\lambda_1 \approx -\left(P_{21} + P_{31} + \frac{1}{2}\omega_2^2/P_{23}\right),$$
$$\lambda_2 \approx -2P_{23}, \quad \lambda_{3,4} = \pm i\omega_1 + P_{11}. \tag{4.6}$$

In accordance with (4.2), the line intensities are given by the expressions

$$A_1 \approx \frac{e^{-\Delta/T}}{1 + e^{-\Delta/T}},$$
$$A_2 \approx -\frac{1}{4}\frac{\omega_2^2}{P_{23}^2}\frac{e^{-\Delta/T}}{1 + e^{-\Delta/T}}, \quad A_{3,4} = \frac{1}{2}\frac{1}{1 + e^{-\Delta/T}}. \tag{4.7}$$

From (4.6) and (4.7) it follows that at low temperatures there is a clear flag pattern of the hyperfine structure (the last two roots of (4.6) give the same flag pattern), corresponding to the frequencies $\omega_1(M,I)$ (cf. formula (4.1)). As the temperature is increased, in addition to this structure there appears an unsplit narrow line (root λ_1) with intensity A_1. For $T \sim \Delta$ the integral intensity of this line becomes of the same order as the intensity of the lines in the flag pattern, or even exceeds it if the flag pattern contains a large number of lines. The root λ_2 gives a broad line of very low intensity A_2, and therefore this term in (4.1) gives practically no contribution to the spectral density.

We note that from (4.6) it follows that the width of the narrow line can either increase or decrease with temperature. (For a definite relation between the parameters, an initial narrowing may be replaced by a broadening of the line.)

B. Let us consider a normal population of levels and, as in the preceding case assume that $P_{14} \gg \omega_1\omega_2$, while all other elements P_{ik} are small compared to ω_1, ω_2. We then have for the roots of (4.3),

$$\lambda_1 \approx -(P_{12} + P_{13} + \omega_1^2/2P_{14}),$$
$$\lambda_2 \approx -2P_{14}, \quad \lambda_{3,4} \approx \pm i\omega_2 + P_{22}. \tag{4.8}$$

The intensities are, respectively,

$$A_1 = \frac{1}{1 + e^{-\Delta/T}},$$
$$A_2 = -\frac{1}{4}\frac{\omega_1^2}{P_{14}^2}\frac{1}{1 + e^{-\Delta/T}}, \quad A_{3,4} = \frac{1}{2}\frac{e^{-\Delta/T}}{1 + e^{-\Delta/T}}. \tag{4.9}$$

According to these formulas we have the reverse picture—at low temperatures only the narrow line (root λ_1) appears, while with increasing temperature the flag pattern of the hyperfine structure appears. (Again the width of the narrow line may either increase or decrease with temperature.) It is interesting to note that if the hyperfine structure is not resolved experimentally, this case leads to an apparent broadening of the line which may be very large.

C. Let us go on the case where the probabilities of horizontal transitions (P_{14}, P_{23}) are small compared to the probabilities of vertical transitions ($P_{12} = P_{43}$). In general this situation is not exceptional. In fact if we limit ourselves to one-phonon transitions, the probability for a strict horizontal transition becomes zero because of the vanishing of the phase volume. Therefore, over the temperature range where the probabilities of two-phonon transitions are small, the probability P_{12} may considerably exceed P_{14} and P_{23}.

For simplicity we consider the case where

$$P_{12} \gg \omega_1, \quad \omega_2 \gg P_{13}, \qquad P_{14} = P_{23} = 0. \quad (4.10)$$

The roots of (4.3) then have the form

$$\lambda_{1,2} \approx -(P_{12} + P_{21}),$$
$$\lambda_{3,4} \approx \pm i\bar{\omega} - \frac{(\omega_1 - \omega_2)^2}{P_{21} + P_{12}} \frac{P_{12}P_{21}}{(P_{12} + P_{21})^2}, \quad (4.11)$$

where

$$\bar{\omega} = \frac{\omega_1 P_{21} + \omega_2 P_{12}}{P_{12} + P_{21}} = \frac{\omega_1 + e^{-\Delta/T}\omega_2}{1 + e^{-\Delta/T}}. \quad (4.12)$$

For the intensities we have

$$A_{1,2} \sim (\omega_1/P_{21})^2, \quad (\omega_2/P_{21})^2; \qquad A_{3,4} \approx 1/2. \quad (4.13)$$

An important conclusion follows from (4.11)–(4.13). It appears that when (4.10) is satisfied there is a temperature range to which there corresponds a single flag in the hyperfine structure, whose frequency changes noticeably with temperature without any significant broadening of the individual lines [roots $\lambda_{3,4}$ in (4.11)]. To the condition $\omega_2 > \omega_1$ there corresponds a spreading of the flag pattern (increase of effective field at the nucleus with increasing temperature), while in the opposite case there is a narrowing.

When $T > \Delta$ the quantity $\bar{\omega}$ emerges onto a plateau corresponding to the value $\bar{\omega} = (\omega_1 + \omega_2)/2$. Such a picture will obviously occur whenever, for $T \sim \Delta$, the element P_{13} becomes small compared to ω_1, ω_2. In the opposite case a marked broadening of the individual lines sets in, which finally leads to the disappearance of the hyperfine structure. In order to make this result clear, we give the roots of (4.3) under the condition that $P_{13} \gtrsim \omega_1, \omega_2$:

$$\lambda_{3,4} = -\frac{P_{13}P_{21} + P_{31}P_{12}}{P_{21} + P_{12}} \pm \left[-\bar{\omega}^2 + \left(\frac{P_{13}P_{21} + P_{31}P_{12}}{P_{21} + P_{12}}\right)^2\right]^{1/2}. \quad (4.14)$$

(For $\lambda_{1,2}$, (4.11) remains valid throughout.)

From this we see that when $P_{13} \sim \bar{\omega}$ there is actually a sizable broadening. With further increase of P_{13}, the lines corresponding to $\lambda_{3,4}$ begin to overlap and then to merge, combining into a single narrow line, in complete agreement with the results of the preceding section.

5. THE CASE OF LARGE ELECTRONIC ANGULAR MOMENTUM

In considering the influence of relaxation processes on the hyperfine structure, an important case is that of large angular momentum of the electron shell. Let us consider the following idealized situation.

Again let us take an expression of the form of

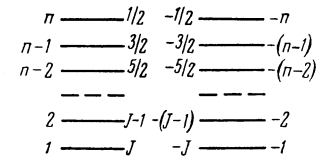

FIG. 4

(3.19) for $\hat{H}_{cr}$. Then, with inverted population of the levels, transitions between the degenerate sublevels ($\pm J_z$) of the lower level will be forbidden because of the very large multipolarity of the transition. This applies also, of course, to all other transitions with large change in J_z, for example, to transitions to levels which are nearest in energy but have the opposite sign for the angular momentum projection. It is clear that in this case there should be a wide range of temperature $\sim J\Delta$ within which there can be a marked change in the hyperfine splitting without any significant broadening of the individual lines.

In order to analyze this problem more directly, let us make various assumptions which do not change the qualitative picture.

1. The angular momentum J of the electron shell is half integral. The electronic levels in the crystal field form $(2J + 1)/2$ equally spaced doublets ($E_{k+1} - E_k = \Delta$). We number these levels as in Fig. 4.

2. In the matrix $\hat{P}$ we neglect all transitions which change the projection of the angular momentum by more than one. For the nonzero elements P_{ij} ($j = i - 1, i, i + 1$) we shall assume that

$$P_{i,i-1} = P_{-i,-i+1} = P. \quad (5.1)$$

In accordance with (3.22),

$$P_{i,i+1} = P_{-i,-i-1} = Pe^{-\Delta/T} = P'. \quad (5.2)$$

We denote the matrix element $P_{n,-n} = P_{-n,n}$ by P_0.

3. We use the expression (3.20) for the Hamiltonian of the hyperfine interaction. We then have for the matrix elements of $\hat{\Omega}$

$$\hat{\Omega}_{kl}(MI) = k|k|^{-1}(n - |k| + 1/2)\,\omega_0\delta_{kl}, \quad \omega_0 = A(M - I). \quad (5.3)$$

If the relation between the parameters P, ω_0, P_0 is such that

$$P \gg \omega_0 \gtrsim P_0, \quad (5.4)$$

one can show that among the eigenvalues of the matrix $-i\hat{\Omega} + \hat{P}$ there are two of order ω_0. They are given by the equation

$$\lambda^2 + 2\gamma\lambda + \omega_{eff}^2 = 0. \quad (5.5)$$

The coefficients γ and ω_{eff} are complicated functions of ω_0, P_0, P and α, where $\alpha = e^{-\Delta/T}$.

Condition 3 allows us to write this dependence analytically:

$$\gamma = \frac{P_0}{1+2\beta}\alpha^{n-1}\frac{1-\alpha}{1-\alpha^n}, \tag{5.6}$$

$$\omega_{\text{eff}}^2 = \frac{\overline{\omega_n^0}}{1+2\beta}(\overline{\omega_n^0} + 2\beta\bar{\omega}_{n-1}), \tag{5.7}$$

where

$$\overline{\omega_n^0} = n\omega_0\left[\frac{1}{1-\alpha^n} - \frac{1+\alpha}{2n(1-\alpha)}\right], \tag{5.8}$$

$$\bar{\omega}_{n-1} = n\omega_0\left[1 + \frac{n-1}{2}\frac{\alpha^{n-1}}{(1-\alpha^n)/(1-\alpha) - n\alpha^{n-1}} - \frac{1+\alpha}{2n(1-\alpha)}\right], \tag{5.9}$$

$$\beta = \frac{P_0}{P}\frac{1}{1-\alpha}\left[1 - n\frac{\alpha^{n-1}(1-\alpha)}{1-\alpha^n}\right]. \tag{5.10}$$

The other eigenvalues are real and of order P, so that they correspond to a smearing of the line. In addition one can show that the intensity of these lines is of order P_0/P, ω_0/P.

For the roots of (5.5) we have

$$\lambda_{1,2} = -\gamma \pm \sqrt{-\omega_{\text{eff}}^2 + \gamma^2}. \tag{5.11}$$

From (5.6) it follows that

$$\gamma \sim e^{-(n-1)\Delta T}.$$

Consequently at low temperatures there is always a clear flag pattern of the hyperfine structure, corresponding to

$$\lambda_{1,2} \approx \pm i\omega_{\text{eff}} - \gamma.$$

Large values of n give a comparatively broad temperature range in which γ remains small and the individual hyperfine structure lines do not fuse, even though ω_{eff}, in accordance with (5.7)–(5.10), changes considerably.

It should be mentioned that when $T \sim n\Delta$, the coefficient γ is $\sim P_0/n$, i.e., it has a value characterizing a line width which is at least n times smaller than the frequency of a horizontal transition. Therefore a well-developed flag pattern will appear over the whole range of temperatures for which

$$P_0/n < \overline{\omega_n^0} \approx n\omega_0/2,$$

i.e.,

$$P_0 \lesssim n^2\omega_0/2. \tag{5.12}$$

When $T > n\Delta$, the hyperfine structure frequencies will reach a plateau. With further rise in temperature, when condition (5.12) is violated, the lines begin to broaden, which results in a rapid disappearance of the hyperfine structure.

[1] The Mössbauer Effect, a collection of papers edited by Yu. Kagan, IIL, 1962.

[2] G. K. Wertheim, Phys. Rev. Letters **4**, 403 (1960).

[3] Nagle, Craig, Barrett, Cochran, Olsen and Taylor, Phys. Rev. **125**, 490 (1962).

[4] Ofer, Avivi, Bauminger, Marinov and Cohen, Phys. Rev. **120**, 406 (1960).

[5] Sklyarevskiĭ, Samoilov and Stepanov, JETP **40**, 1874 (1961), Soviet Phys. JETP **13**, 1360 (1961).

[6] Kalvius, Kienle, Böckmann and Eicher, Z. Physik **163**, 87 (1961).

[7] Wagner, Stanek, Kienle and Eicher, Z. Physik **166**, 1 (1962).

[8] F. Stanek, Z. Physik **166**, 6 (1962).

[9] Cohen, Hauser and Mössbauer, Proc. Second Mössbauer Conference, J. Wiley, New York, 1962, p. 172.

[10] P. W. Anderson, J. Phys. Soc. Japan **9**, 316 (1954).

Translated by M. Hamermesh
265